Electronic supplementary information

PVP-assisted preparation of ferrocenyl metal-organic framework hollow microspheres for *in situ* loading palladium nanoparticles as heterogeneous catalyst

Zheng Deng,[a, b] Yi Guo [b], Zhuoyi Li [b], Xiaobin Wang [b], Xinsheng Peng *[b] and Yu-Jia Zeng *[a]

a: Shenzhen Key Laboratory of Laser Engineering, College of Physics and Optoelectronic Engineering, Shenzhen University, Shenzhen, 518060, P. R. China.

E-mail: yjzeng@szu.edu.cn

b: State Key Laboratory of Silicon Materials, School of Materials Science and Engineering, Zhejiang University, Hangzhou 310027, P.R. China.

E-mail: pengxinsheng@zju.edu.cn.

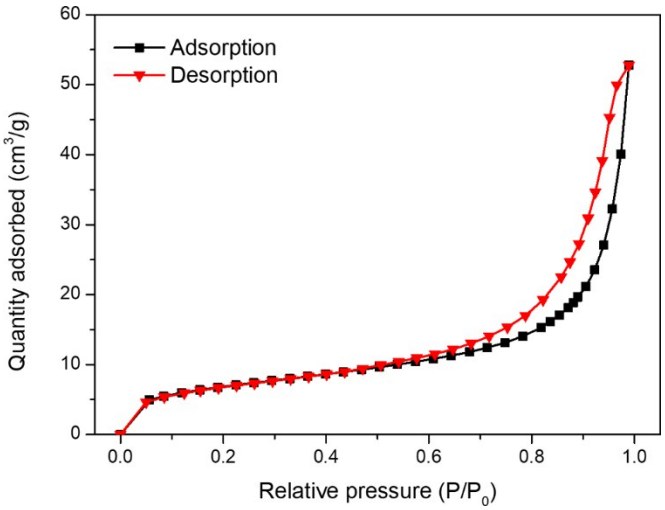

Figure S1. N_2 adsorption and desorption isothermal of Zn-Fc MOF.

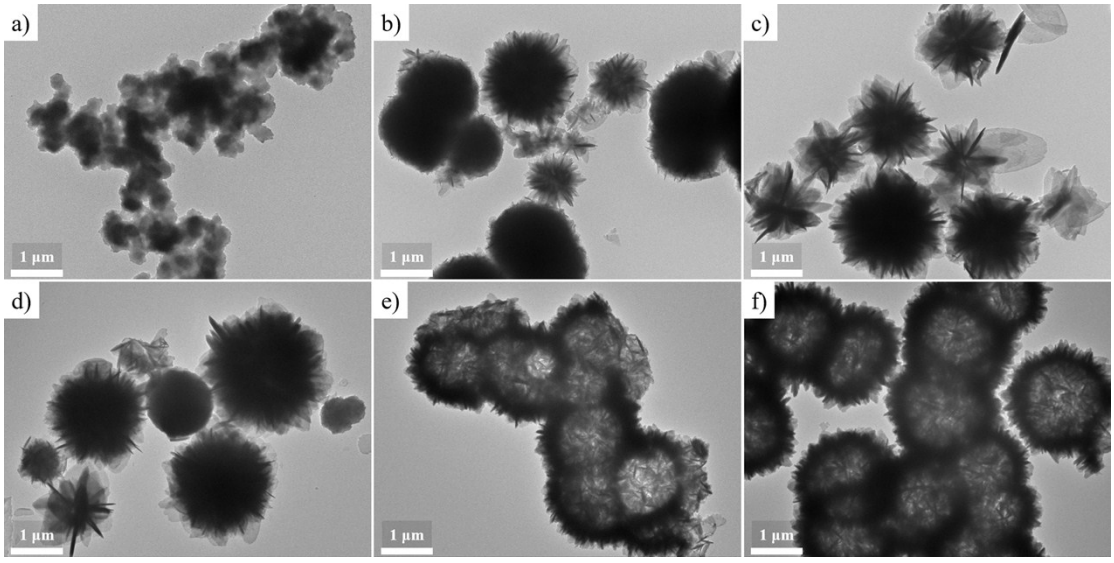

Figure S2. TEM images of Zn-Fc MOF synthesized with addition of different amount of PVP. a) 0 equiv., b) 3 equiv., c) 10 equiv., d) 20 equiv., e) 30 equiv. and f) 40 equiv.

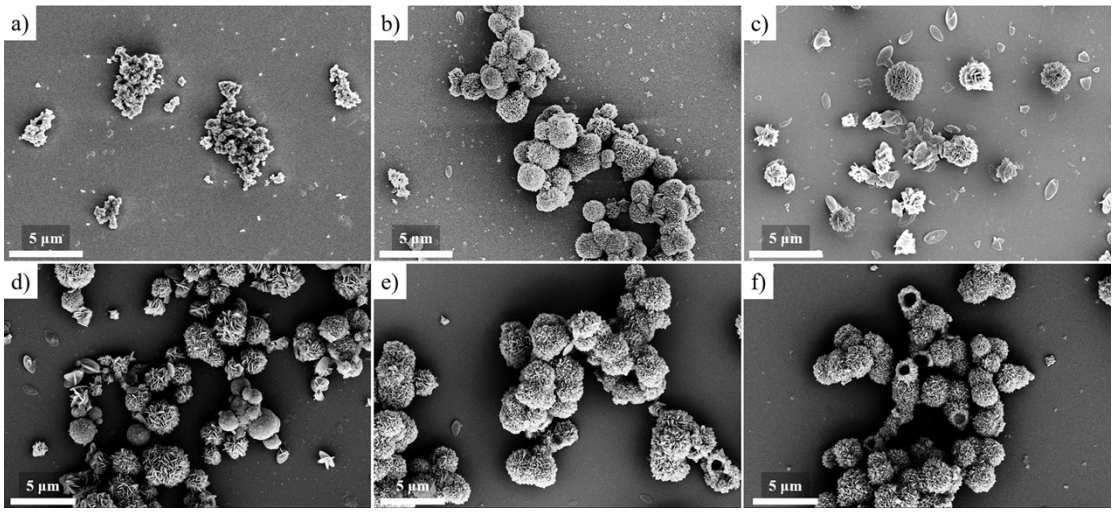

Figure S3. SEM images of Zn-Fc MOF synthesized with addition of different amount of PVP. a) 0 equiv., b) 3 equiv., c) 10 equiv., d) 20 equiv., e) 30 equiv. and f) 40 equiv.

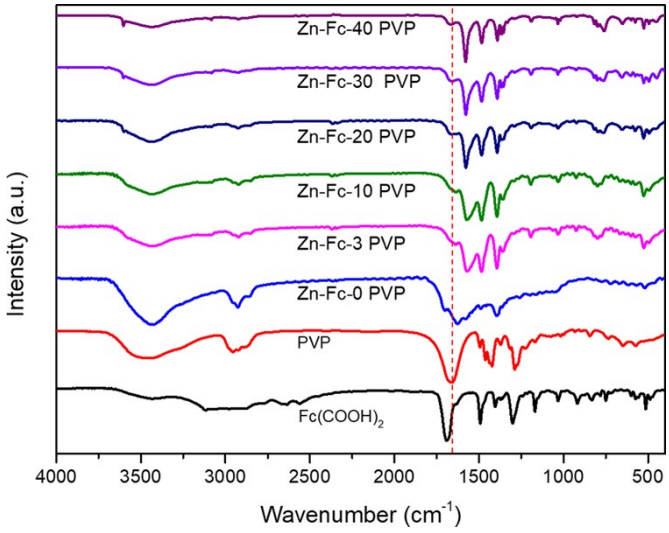

Figure S4. FT-IR spectra of Zn-Fc MOF synthesized with addition of different amount of PVP.

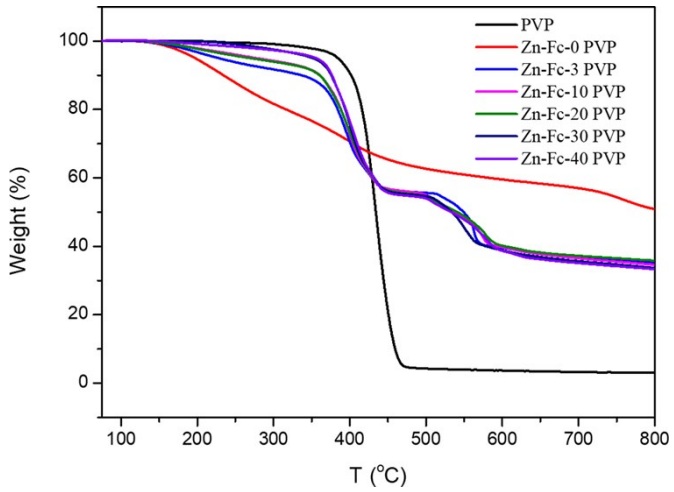

Figure S5. TGA curves of PVP and Zn-Fc MOF synthesized with addition of different amount of PVP.

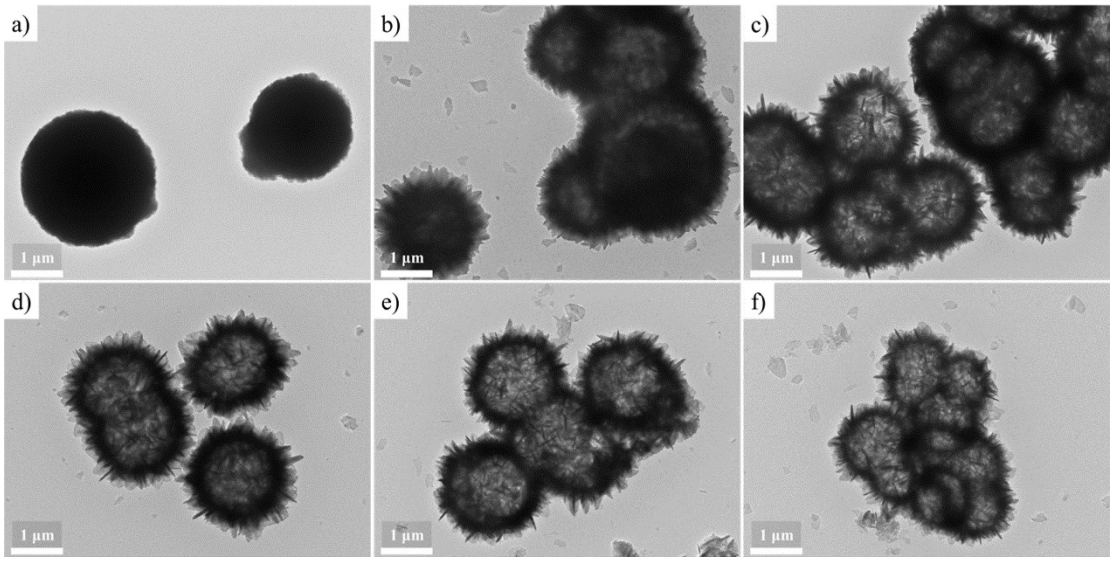

Figure S6. TEM images of Zn-Fc MOF synthesized with addition of 30 equiv. of PVP at different temperature. a) 100 °C, b) 110 °C, c) 120 °C, d) 130 °C, e) 140 °C and f) 150 °C.

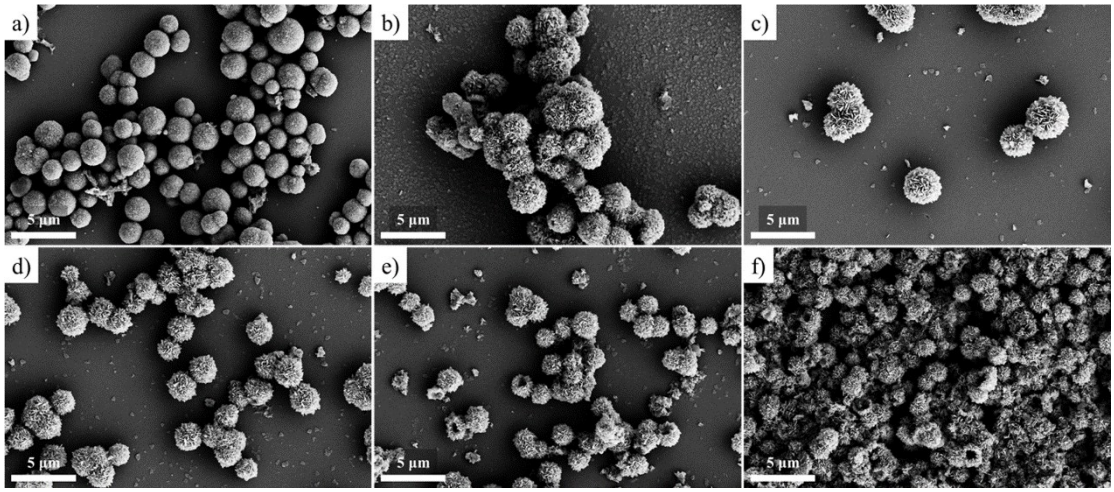

Figure S7. SEM images of Zn-Fc MOF synthesized with addition of 30 equiv. of PVP at different temperature. a) 100 °C, b) 110 °C, c) 120 °C, d) 130 °C, e) 140 °C and f) 150 °C.

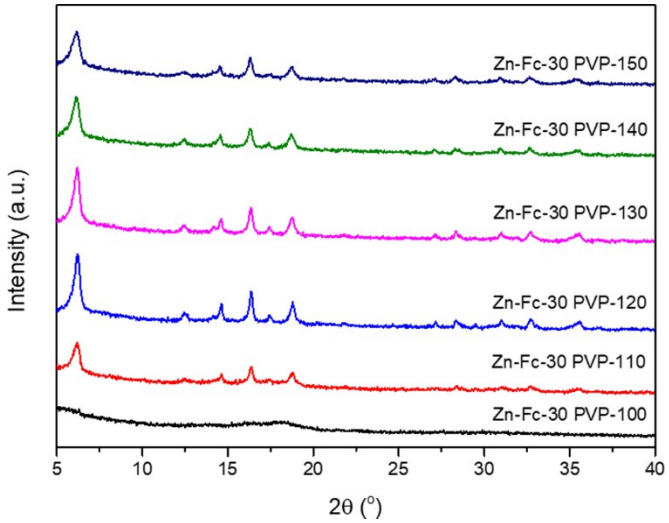

Figure S8. XRD patterns of Zn-Fc MOF synthesized with addition of 30 equiv. of PVP at different temperature.

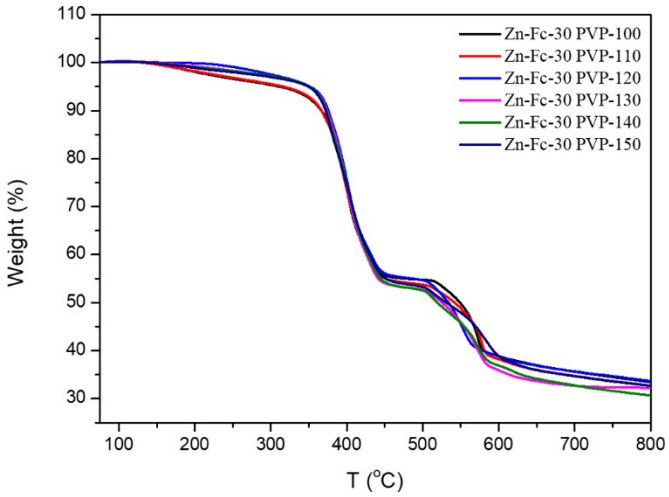

Figure S9. TGA curves of Zn-Fc MOF synthesized with addition of 30 equiv. of PVP at different temperature.

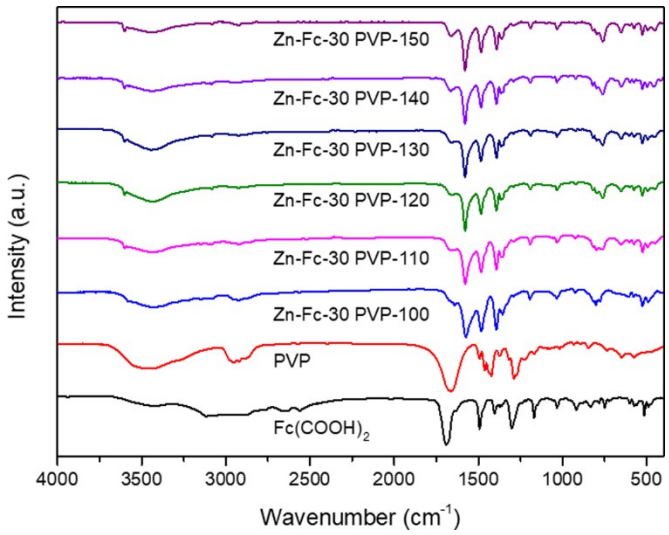

Figure S10. FT-IR spectra of Zn-Fc MOF synthesized with addition of 30 equiv. of PVP at different temperature.

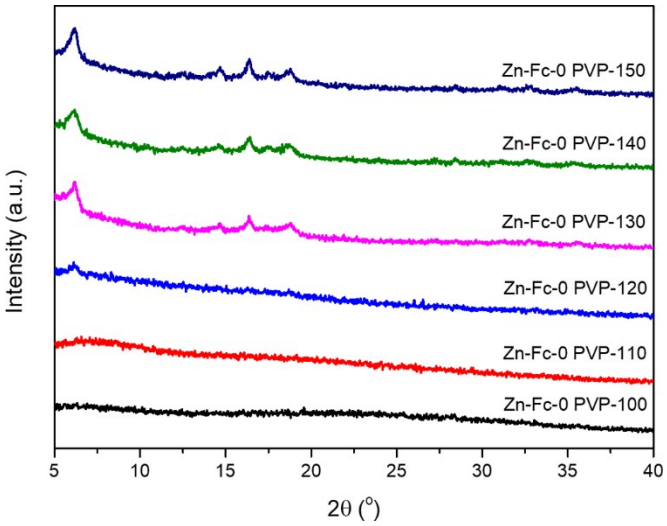

Figure S11. XRD patterns of Zn-Fc MOF synthesized without addition of PVP at different reaction temperature.

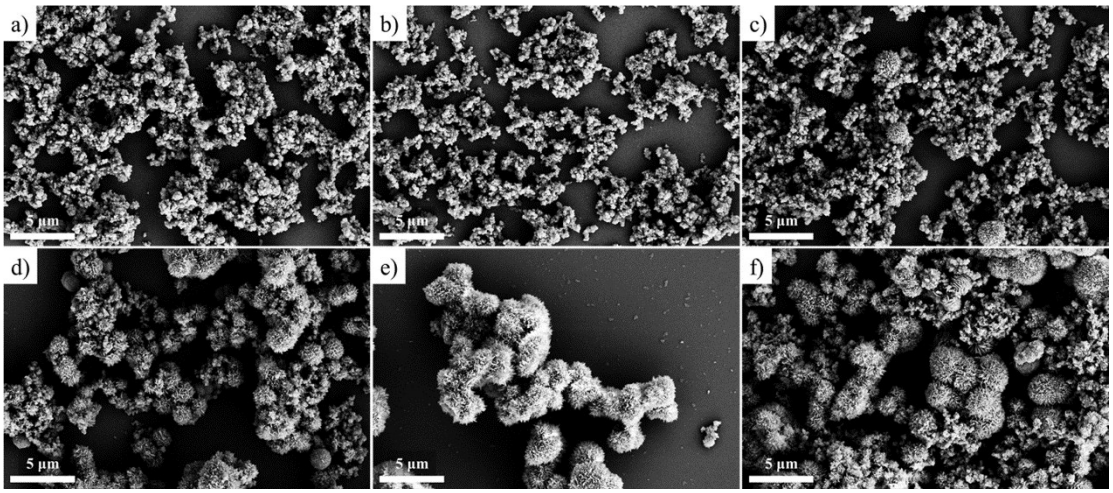

Figure S12. SEM images of Zn-Fc MOF synthesized without addition of PVP at different temperature. a) 100 °C, b) 110 °C, c) 120 °C, d) 130 °C, e) 140 °C and f) 150 °C.

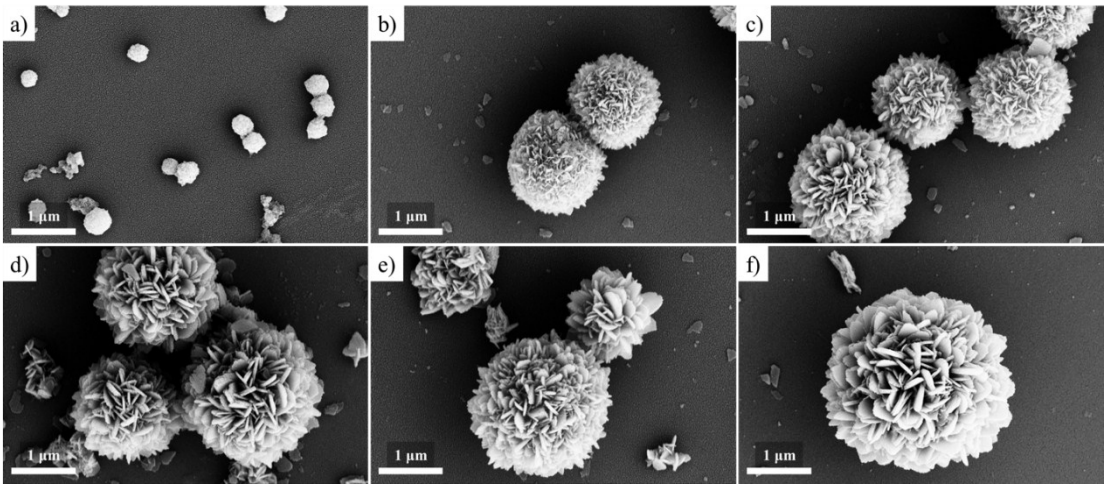

Figure S13. SEM images of Zn-Fc MOF synthesized for different reaction time. a)1h, b) 2h, c) 3h, d) 6h, e) 9h and f) 12h.

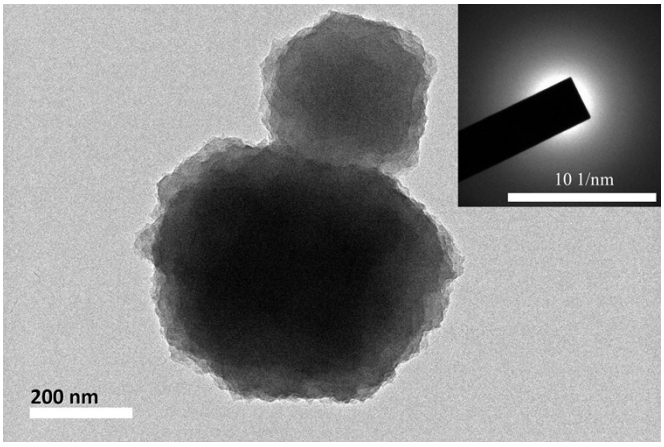

Figure S14. HR-TEM image and electron diffraction image of Zn-Fc-1h.

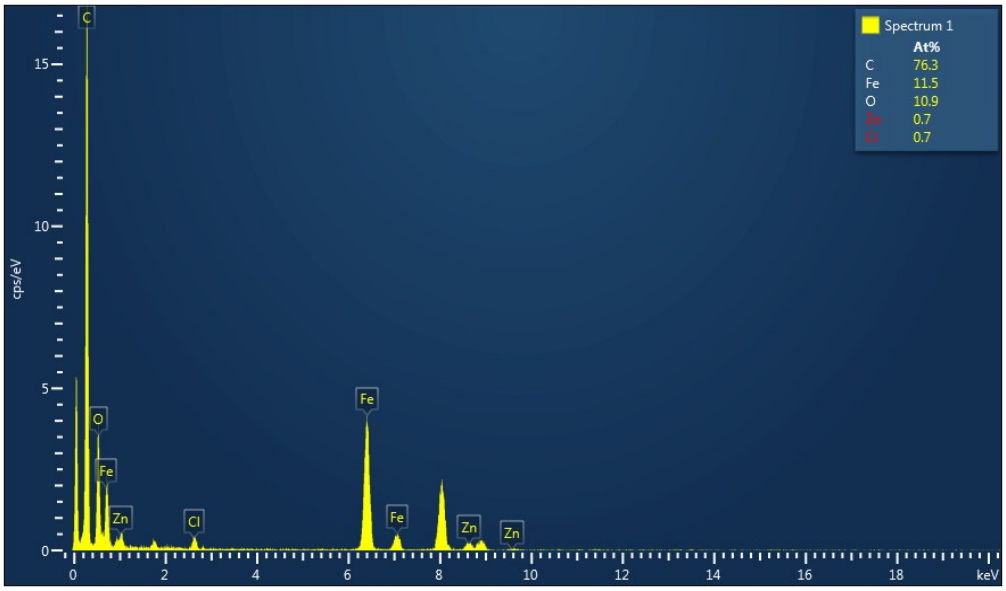

Figure S15. EDS spectrum of Zn-Fc-1h.

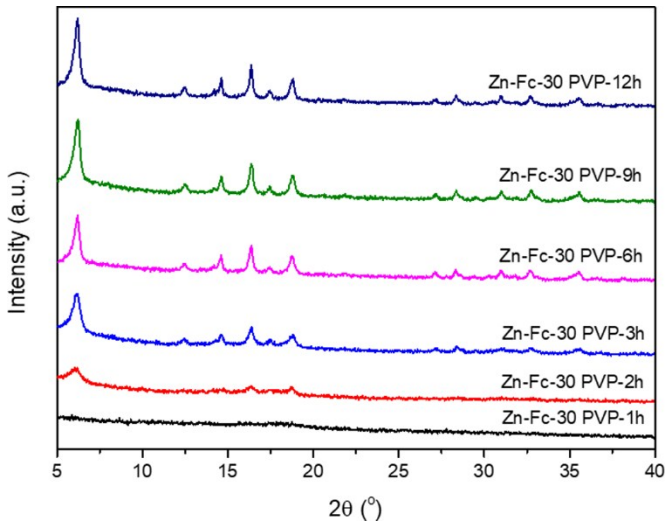

Figure S16. XRD patterns of Zn-Fc MOF synthesized with addition of 30 equiv. of PVP under different reaction time (1-12h).

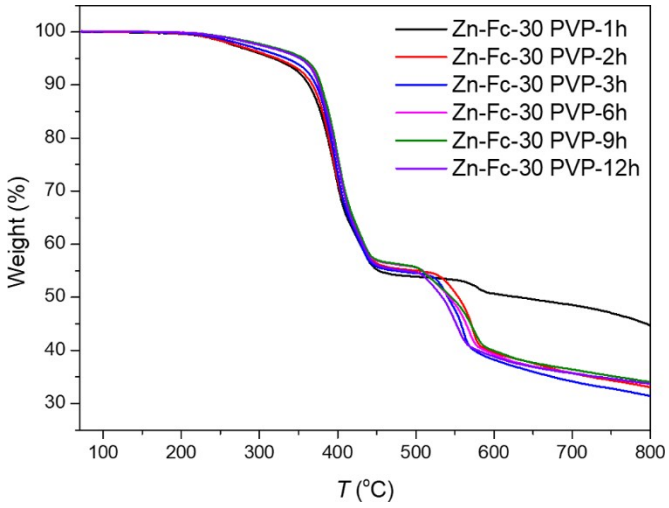

Figure S17. TGA curves of Zn-Fc MOF synthesized with addition of 30 equiv. of PVP under different reaction time (1-12h).

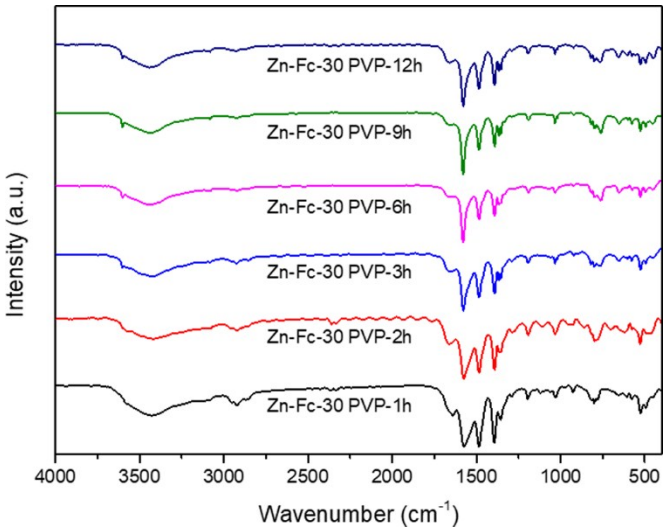

Figure S18. FT-IR spectra of Zn-Fc MOF synthesized with addition of 30 equiv. of PVP under different reaction time (1-12h).

Table S1. Summary of CV data of Zn-Fc MOF hollow microsphere modified electrode obtained at different scanning rate.

v	E_{pa}	E_{pc}	$E_{1/2}$	$\triangle E_p$	i_{pa}	i_{pc}	i_{pa}/i_{pc}
V/s	V	V	V	V	μA	μA	
0.1	0.955	0.725	0.840	0.230	2.186	1.919	1.14
0.2	0.952	0.728	0.840	0.224	3.186	2.847	1.12
0.3	0.944	0.728	0.836	0.216	4.017	3.554	1.13
0.4	0.950	0.725	0.838	0.225	4.806	4.187	1.15
0.5	0.949	0.733	0.841	0.216	5.487	4.768	1.15

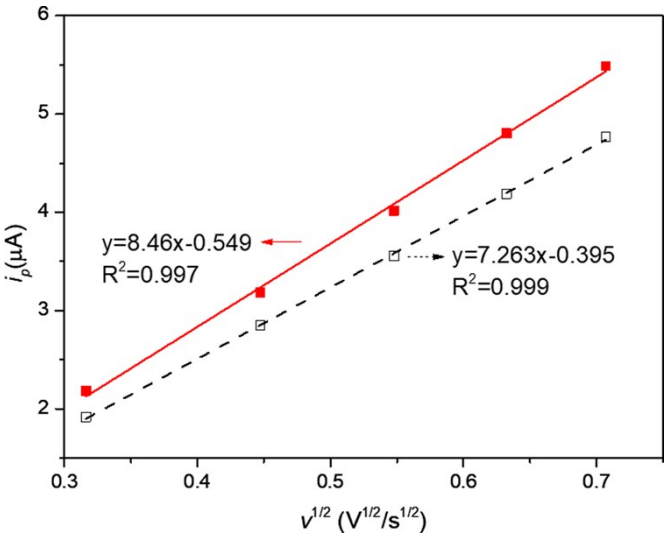

Figure S19. Liner fitting curves of i_{pa} (solid line) and i_{pc} (dashed line) to $v^{1/2}$.

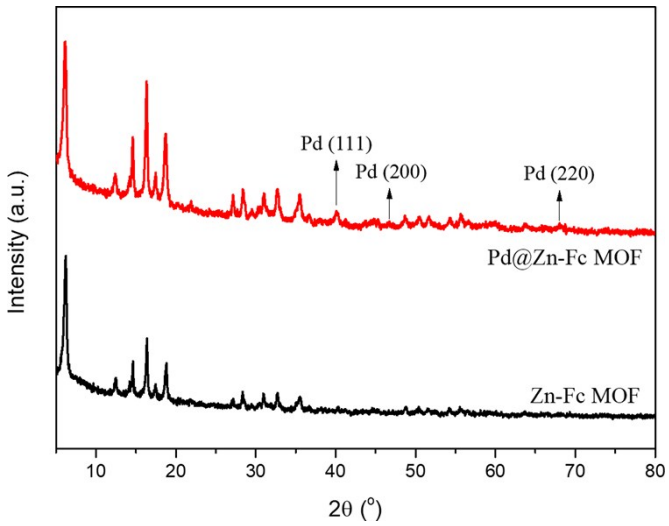

Figure S20. XRD patterns of Zn-Fc MOF and Pd@Zn-Fc MOF.

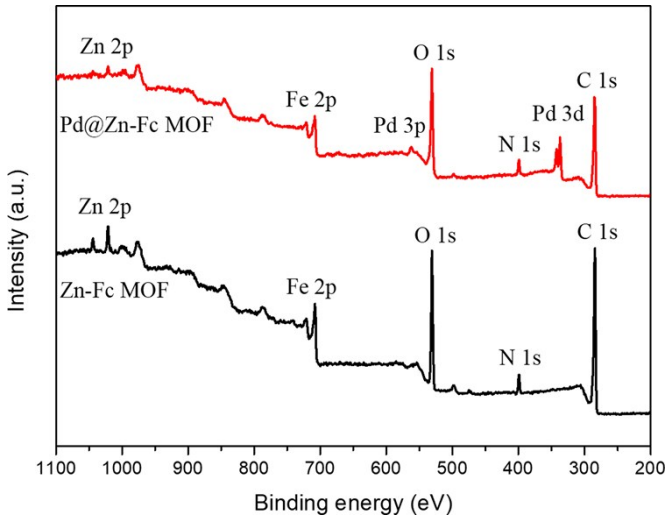

Figure S21. XPS spectra of Zn-Fc MOF and Pd@Zn-Fc MOF

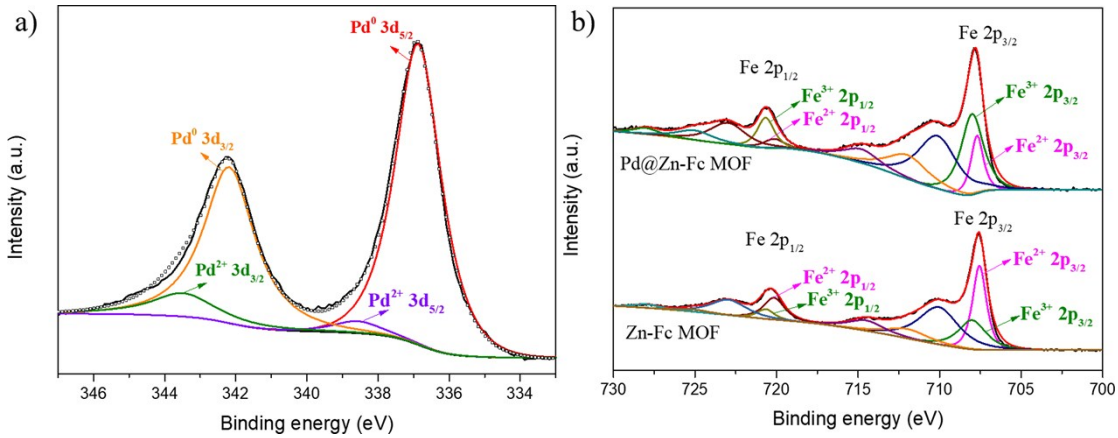

Figure S22. a) XPS spectrum of Pd 3d in Pd@Zn-Fc MOF and b) XPS spectra of Fe 2p in both Zn-Fc MOF and Pd@Zn-Fc MOF.

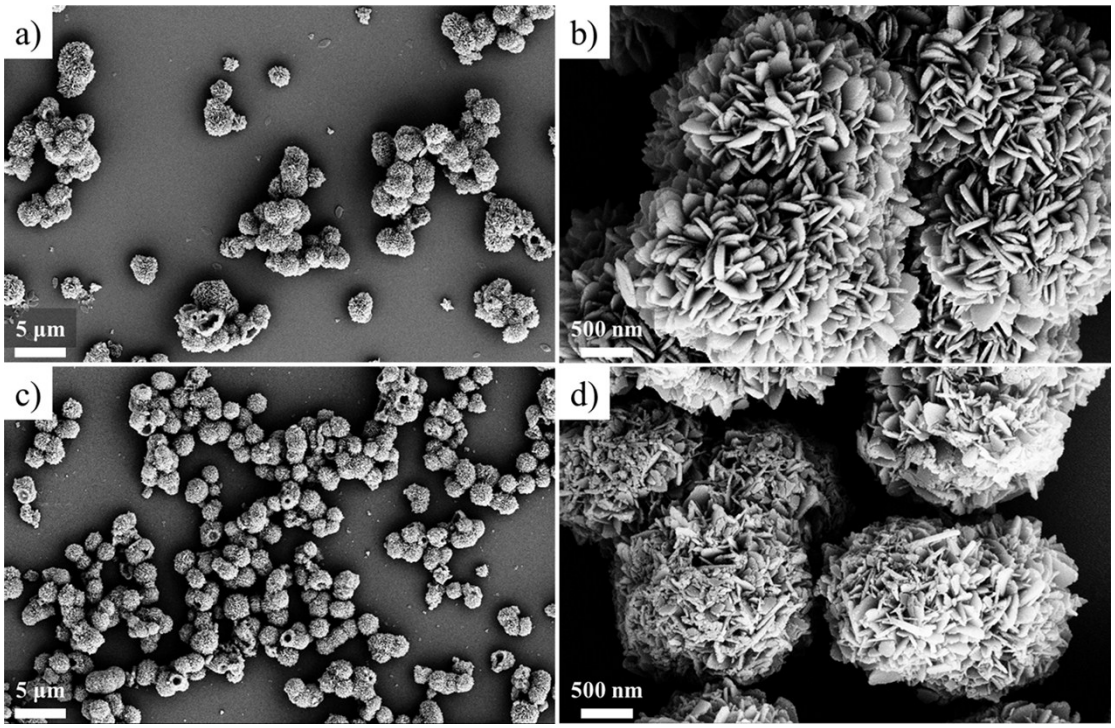

Figure S23. SEM images of Zn-Fc MOF (a, b) and Pd@Zn-Fc MOF (c, d).

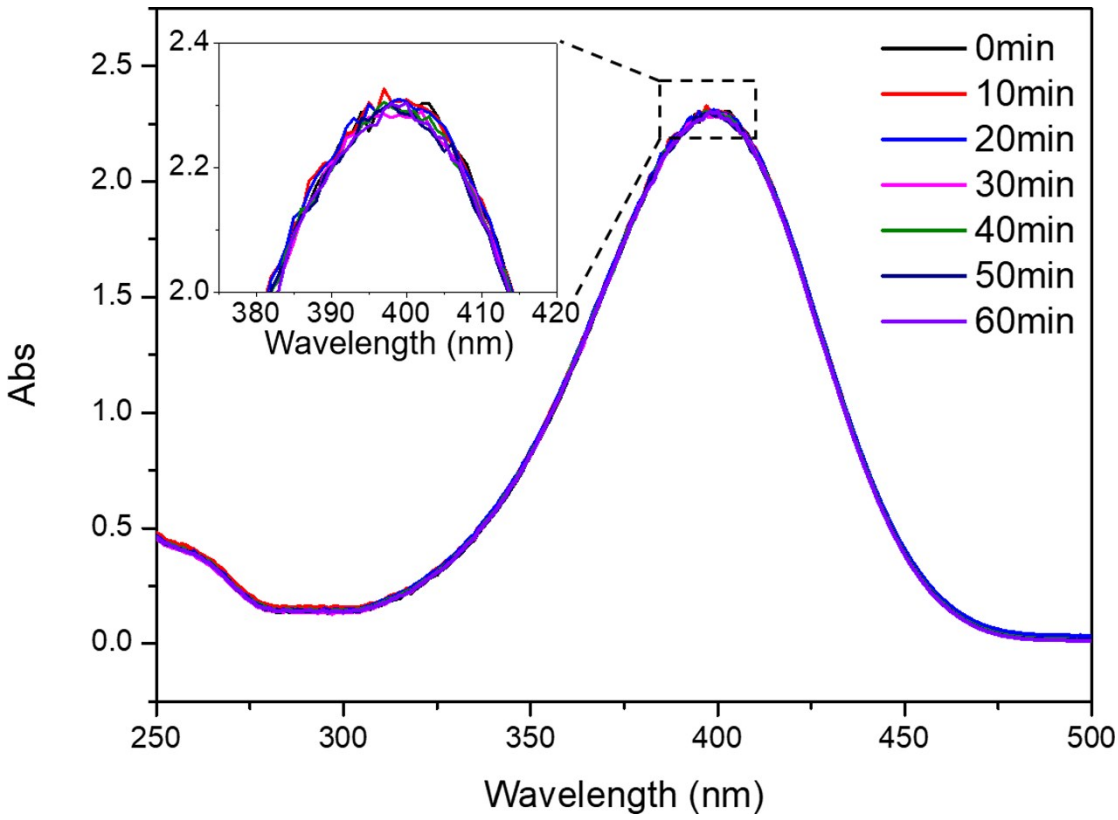

Figure S24. UV-vis spectra of the reaction solution taken at different reaction time without adding Pd@Zn-Fc MOF as a catalyst.

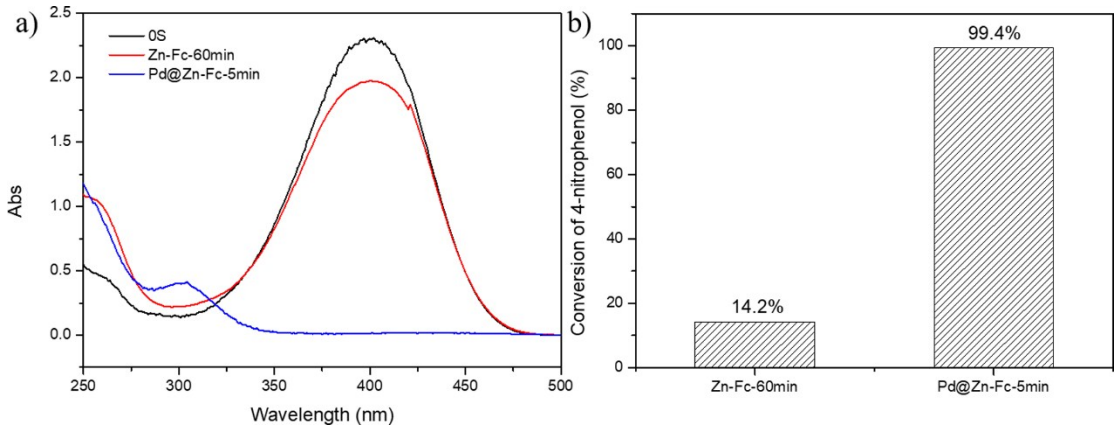

Figure S25. a) UV-vis spectra of the initial solution and reaction solution using Zn-Fc MOF and Pd@Zn-Fc MOF as catalyst respectively after different reaction time. b) Conversion of 4-nitrophenol catalyzed by Zn-Fc MOF and Pd@Zn-Fc MOF after different reaction time.

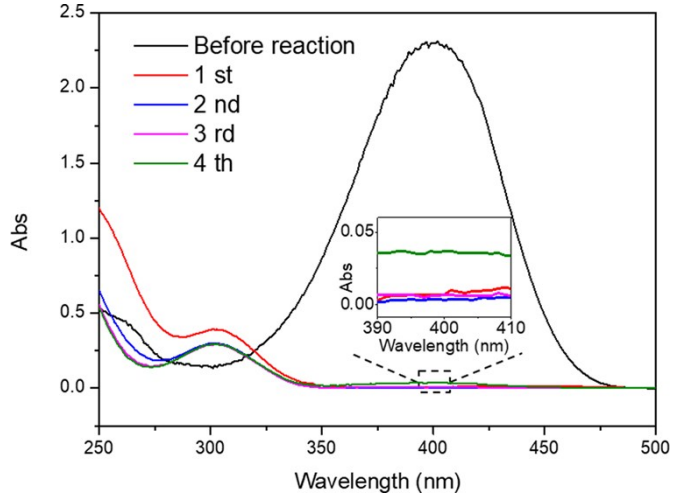

Figure S26. UV-vis spectra of reaction solution taken after different recycle times.

Table S2. Comparison of the rate constant (k) of 4-nitrophenol reduction catalyzed by Pd loaded on different type of supports.

Supports	k/$S^{-1}\times10^2$	Ref
Fe_xO_y@mesoporous SiO_2	0.16	1
Graphene	0.235	2
Dendrimer	0.4	3
SPB	0.441	4
CNT/PiHP	0.5	5
CeO_2	0.8	6
Fe_3O_4@SiO_2@CeO_2	1.05	7
CNTs	1.05	8
SBA-15	1.18	9
Ppy/TiO_2	1.22	10
Fe_3O_4@CeO_2	1.6	7
Zn-Fc MOF hollow microspheres	1.82	This work

References:

1. T. Yao, T. Cui, X. Fang, F. Cui and J. Wu, *Nanoscale*, 2013, 5, 5896-5904.
2. Z. Wang, C. Xu, G. Gao and X. Li, *RSC Adv.*, 2014, 4, 13644-13651.
3. C. Deraedt, L. Salmon and D. Astruc, *Adv. Synth. Catal.*, 2014, 356, 2525-2538.
4. Y. Mei, Y. Lu, F. Polzer, M. Ballauff and M. Drechsler, *Chem. Mater.*, 2007, 19, 1062-1069.
5. H. Li, L. Han, J. Cooper-White and I. Kim, *Green Chem.*, 2012, 14, 586-591.
6. B. Liu, S. Yu, Q. Wang, W. Hu, P. Jing, Y. Liu, W. Jia, Y. Liu, L. Liu and J. Zhang, *Chem. Commun.*, 2013, 49, 3757-3759.

7. Q. Wang, W. Jia, B. Liu, A. Dong, X. Gong, C. Li, P. Jing, Y. Li, G. Xu and J. Zhang, *J. Mater. Chem. A*, 2013, 1, 12732-12741.
8. X. Gu, W. Qi, X. Xu, Z. Sun, L. Zhang, W. Liu, X. Pan and D. Su, *Nanoscale*, 2014, 6, 6609-6616.
9. J. Morere, M. J. Tenorio, M. J. Torralvo, C. Pando, J. A. R. Renuncio and A. Cabanas, *J. Supercrit. Fluids*, 2011, 56, 213-222.
10. X. Lu, X. Bian, G. Nie, C. Zhang, C. Wang and Y. Wei, *J. Mater. Chem.*, 2012, 22, 12723-12730.